

Static and dynamic light scattering by aqueous polyelectrolyte solutions: effect of molecular weight, charge density and added salt*

Stephan Förster and Manfred Schmidt†

Max-Planck-Institut für Polymerforschung, Ackermannweg 10, D-6500 Mainz, FRG

and Markus Antonietti

Institut für Physikalische Chemie der Universität Mainz, Jakob-Welder-Weg 15, D-6500 Mainz, FRG

(Received 15 November 1989; accepted 18 December 1989)

Aqueous solutions of quaternized poly(2-vinylpyridine) were investigated by static (SLS) and dynamic (DLS) light scattering over a wide range of polyelectrolyte, c_{pe} , and salt concentrations, c_s ($10^{-3} \leq c_{pe} \leq 10^2 \text{ g l}^{-1}$, $10^{-5.5} \leq c_s \leq 10^{-1} \text{ mol l}^{-1}$). Using DLS the cooperative diffusion coefficient D was measured as a function of c_{pe} and c_s . D exhibits a characteristic behaviour in each of three different concentration regimes. In the 'dilute lattice' regime, where $\lambda = c_{pe}/c_s \ll 1$, one diffusion coefficient is observed. In the transition regime, where $\lambda \approx 1$, D increases with increasing polyelectrolyte concentration and a slow diffusive mode gradually appears. For $\lambda \gg 1$ ('semidilute lattice regime') a fast diffusive process, which is interpreted as the gel mode of a transient network, and a slow diffusive process, which is associated with long-range concentration fluctuations, are observed. For the dynamic behaviour, the absolute ionic strength of the solution is only of minor importance.

(Keywords: static and dynamic light scattering; small-angle neutron scattering; aqueous polyelectrolyte solutions; diffusion; temporary cluster; plasmon mode)

INTRODUCTION

Although the exceptional behaviour of polyelectrolytes in solution is a matter of considerable scientific and technological interest, a complete understanding on a molecular basis is still missing¹. Obviously, the combination of both polymer and electrolyte properties results in high complexity.

For polyelectrolyte solutions *without added salt* it is generally accepted that a highly charged polyelectrolyte chain at very high dilution is nearly fully stretched due to the strong electrostatic repulsion of the like charges along the chain. This feature was used in a theoretical approach by Katchalsky², where the polyelectrolytes are represented as rigid, uniformly charged rods, arranged in a parallel close-packed array. This simple model is, however, not suitable to provide an understanding of the behaviour of polyelectrolyte solutions at higher concentrations. De Gennes *et al.*³ applied scaling concepts to extend the theoretical description to semidilute solutions. They distinguish three different concentration regimes, each having a different polyion behaviour, defined by the absolute ionic strength of the solution. At the lowest concentrations (dilute regime), the polyelectrolyte chains are on average widely separated and fully stretched. Above a certain critical concentration the fully stretched

chains cannot orient freely any more and the electrostatic interaction between the polyions is expected to lead to a three-dimensional periodic lattice. At much higher concentrations, where the chains overlap considerably, the formation of a transient network with a characteristic correlation length ξ is suggested, similar to the case of flexible neutral polymers. Odijk⁴ and Skolnick and Fixman⁵ developed an explanation for the concentration-dependent flexibility of polyelectrolyte chains by taking into account the counterion screening of the charges on the macromolecule when calculating its persistence length using the worm-like chain model. This theory led to a refinement of the de Gennes theory by Odijk⁶, who considered additional concentration regimes. Based on Odijk's approach and on calculations of the persistence length by Le Bret⁷, Kaji *et al.*⁸ proposed a phase diagram for aqueous polyelectrolyte solutions without added salt dependent on the degree of polymerization and on the polymer concentration, which classified several concentration regimes. It should be mentioned that, besides scaling arguments, there are also other theoretical approaches to the properties of polyelectrolyte solutions, including the projection operator technique⁹ and the mode-mode coupling approximation^{10,11}.

Static and dynamic light scattering (SLS, DLS) experiments have revealed an even more complex picture of the properties of polyelectrolytes in solution, which cannot be fully explained within the framework of the scaling approach. Grüner and Lehmann¹² investigated

* Dedicated to Professor Walther Burchard on the occasion of his 60th birthday

† To whom correspondence should be addressed

sodium poly(styrene sulphonate), NaPSS, of molecular weight $M_w = 100\,000\text{ g mol}^{-1}$ at concentrations $10^{-3} < c_{pe} < 10^3\text{ g l}^{-1}$, spanning the dilute, semidilute and concentrated regimes. At high dilution they measured a concentration-independent diffusion coefficient, which was interpreted as the diffusion of single rigid rods. In the semidilute regime the diffusion coefficient scaled approximately with $c^{1/2}$, as was theoretically predicted by Odijk⁶. At higher concentrations a concentration-independent diffusion was again observed, in contradiction to Odijk's theory. Unfortunately, neither the static scattering intensity nor the angular dependence of the first cumulant was recorded, which would be needed to identify the formation of a polyion lattice. Those quantities were, however, studied by Drifford and Dalbiez¹³ for NaPSS with $M_w = 780\,000\text{ g mol}^{-1}$. They found a peak in the static scattering function $I(q)$ at a wavevector q which varied as $c^{1/2}$. Coinciding with this maximum in the scattering intensity, a minimum of the diffusion coefficient was observed as evaluated from a cumulant analysis of the correlation function. In the semidilute regime Drifford and Dalbiez observed a decreasing diffusion coefficient with increasing concentration, in contradiction with the results of Grüner and Lehmann¹². However, the decrease was in agreement with Koene and Mandel¹⁴, who studied NaPSS of the same molecular weight, but only in the semidilute and concentrated regimes.

In the semidilute regime Koene and Mandel¹⁴ report a 'slow' diffusion. The corresponding diffusion coefficient decreases with increasing concentration and with increasing molecular weight. At higher concentration a 'fast' diffusion coefficient was observed, which was independent of concentration and molecular weight. An interpretation based on a reptation model has been proposed for the slow diffusion mechanism. The fast diffusion was explained by a 'cooperative' motion of the entangled network. It was, however, not clear whether or not both diffusion processes occur simultaneously over a wider concentration range.

Konak *et al.*¹⁵ investigated poly(methacrylic acid) of molecular weights 30 000 and 400 000 g mol^{-1} at various degrees of neutralization α , by dynamic light scattering. At low α , only a short time decay of the autocorrelation function is observed. When $\alpha \gg 0$, a second, much slower, process becomes noticeable. The fast diffusion was attributed to a cooperative diffusion of polyions and counterions and the slow process to the diffusion of interchain domains (clusters). Both diffusive modes cannot be explained within the framework of the scaling approach as proposed by de Gennes³ and Odijk⁶.

Schmidt¹⁶ investigated quaternized poly-2-vinylpyridine) over a wide range of concentrations. He demonstrated that both fast and slow diffusion occur simultaneously in semidilute polyelectrolyte solutions. The results elucidated the apparent contradiction between the experiments of Grüner and Lehmann¹², who only observed the fast mode, and of Koene and Mandel¹⁴, who observed the slow mode at small concentrations and the fast mode at higher concentrations. Schmidt concluded that clusters of almost uniform size are formed in aqueous polyelectrolyte solutions without added salt, the diffusion of which represents the slow diffusive process. Recent results of Schlager and Burchard^{17,18} on a different polyelectrolyte system show qualitatively the same dynamic behaviour.

Small-angle neutron scattering (SANS) experiments on semidilute solutions of NaPSS have been performed to elucidate the structural and dynamic properties of polyelectrolyte solutions without added salt^{19–21}. The scattering curves are characterized by a broad maximum at a scattering vector q_m , which is proportional to $c_{pe}^{1/2}$. The persistence length l_p , which could be determined by a special deuterium labelling technique²⁰, also exhibits the $c_{pe}^{1/2}$ dependence. A constant relation between the static correlation length ξ , defined as $2\pi q_m^{-1}$, and the total persistence length of a single polymer chain was experimentally established. The data were interpreted in terms of a two-dimensional close-packed structure of flexible segments of a few persistence lengths.

Theoretically, the addition of low-molecular-weight electrolyte changes the polyelectrolyte properties considerably. In the case of flexible polyelectrolytes, it is current opinion that the presence of salt screens the electrostatic interaction and that eventually at high salt concentration the chains behave similarly to flexible neutral macromolecules. Dynamic light scattering studies, however, reveal a somewhat bizarre behaviour of the dynamics of polyelectrolytes as a function of added salt. Schurr *et al.*²² observed in a series of dynamic light scattering studies on a poly(L-lysine) hydrobromide a complicated change in the diffusion coefficient D as a function of salt concentration. After a slight initial rise as the salt concentration was decreased, D drops precipitously by over an order of magnitude within a small change in added salt concentration. This phenomenon was referred to as an 'ordinary–extraordinary' phase transition. The changes in D appeared sufficiently sharp such that a critical salt concentration could be defined. Experimental investigations of other groups on poly(L-lysine)^{23,24}, deoxyribonucleic acid (DNA)^{25,26} and bovine serum albumin (BSA)²⁷ show qualitatively the same results. Drifford and Dalbiez²⁸ performed similar studies on NaPSS and derived an empirical relationship for the critical concentration as a function of the ratio c_{pe}/c_s .

The concentration dependence of the reduced viscosity of salt-free polyelectrolyte solutions exhibits an unusual behaviour because it increases with decreasing polyelectrolyte concentration^{29,30}. Qualitatively, this was explained by a coil-to-rod transition of the polyions upon dilution due to the increasing electrostatic interactions along the chains with decreasing ionic strength. Careful but still controversial investigations of the dilute-solution

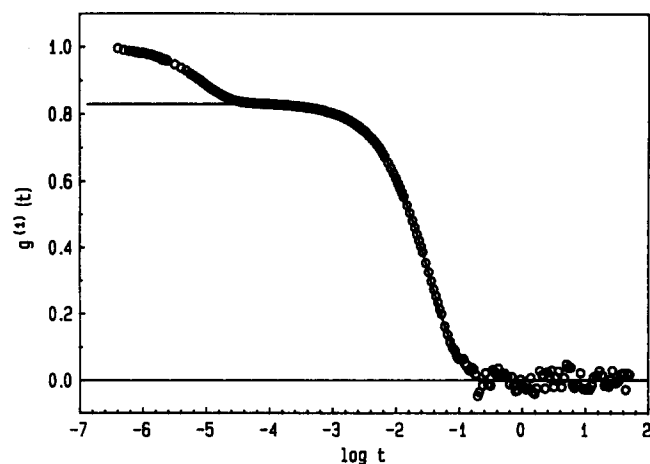
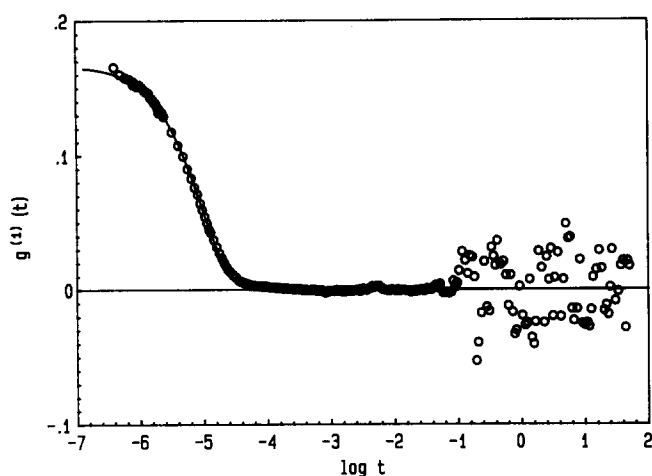
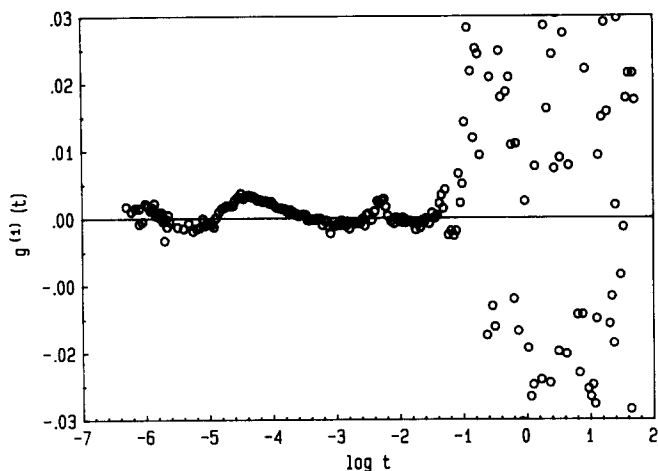


Figure 1 Fit of the slow mode

Table 1 Some characteristic properties of the polyelectrolyte samples. L is the contour length of the polymer, Q the degree of quaternization and b the average distance between two successive charges on the chain

Samples	M_w (g mol ⁻¹)	L (Å)	Q (mol%)	M_w/M_n	b (Å)
P1Q1	580 000	8300	40	1.10	6.3
P1Q2	780 000	8300	75	1.10	3.3
P3Q3	200 000	1800	98	1.10	2.6
P4Q1	109 000	1300	65	1.04	3.8
P5Q1	2 260 000	20500	100	1.30	2.5

**Figure 2** Fit of the fast mode**Figure 3** Final residues

behaviour^{11,31,32} reveal that the rise of the reduced viscosity is always followed by a maximum with a subsequent steep decrease at the lowest concentrations. The concentration where the maximum is observed is independent of molecular weight and depends only on the ratio c_{pe}/c_s . Rabin¹¹ derived a theoretical expression for the viscosity of such solutions, assuming that the hydrodynamics of low-ionic-strength polyelectrolyte solutions is dominated by the electrostatic repulsion between the polyions.

As outlined above, the various experimental results on polyelectrolytes with and without added salt are currently poorly understood. Following the light scattering experiments on quaternized poly(2-vinylpyridine) of Schmidt¹⁶, we wish to add an experimental study investigating the influence of charge density and molecular weight on the static and dynamic behaviour of polyelectrolytes in aqueous solutions with and without added salt.

EXPERIMENTAL

Synthesis of poly(N-benzyl-2-vinylpyridinium bromide)

2-Vinylpyridine (Aldrich) was polymerized anionically using standard techniques³³. The poly(2-vinylpyridine) obtained was carefully characterized by static and dynamic light scattering in tetrahydrofuran (THF) and by g.p.c. in dimethylformamide (DMF)³⁴. All polymers exhibited a narrow molecular-weight distribution ($M_w/M_n \leq 1.1$, except for the highest molecular weight). The molecular weights varied between 50 000 and 1 000 000 g mol⁻¹, which corresponds to contour lengths between 1300 and 20 500 Å (Table 1).

Quaternization was achieved by allowing a 2% solution poly(2-vinylpyridine) in benzyl bromide/nitromethane (1:3) to stand in the dark at room temperature for four weeks. Afterwards, the polymer was completely quaternized as tested by elemental analysis and counterion titration. Shorter reaction times yielded polyelectrolytes with lower degree of quaternization. After the reaction the solution was concentrated by the evaporation of solvent. The solution was then poured dropwise into toluene, where the polyelectrolyte precipitated. The precipitate was removed by filtration and washed three times with petroleum ether. Further purification was achieved by dissolution in a methanol/ethanol mixture and subsequent precipitation in ethyl acetate/toluene (1:1). This procedure was repeated, usually three times, until a colourless polymer was obtained. Afterwards the polymer was dissolved in deionized water, filtered and freeze-dried.

The degree of quaternization was calculated from the Br/N ratio, which was determined by elemental analysis and counterion titration. The polyelectrolytes were also characterized by aqueous g.p.c.³⁵. According to the g.p.c. measurements, the molecular-weight distributions were not noticeably changed during the quaternization reaction.

It should be pointed out that the strategy for this synthesis completely rules out the presence of low-molecular-weight electrolyte impurities in the polyelectrolyte. This is of particular importance when the experiments are performed under *salt-free* conditions.

At constant polyion concentration the total ionic strength of the solutions was varied by addition of potassium bromide (Merck Spectrograde) which is referred to as 'added salt' throughout the paper.

Light scattering

Light scattering measurements were performed with a commercially available spectrometer consisting of an ALV-SP81 goniometer and an ALV-3000 correlator. A Kr-ion laser (Spectra Physics, model 2025) operating at 647.1 nm wavelength was used as the light source. Most of the correlation functions were recorded in the real-time

'multi tau' mode in which the time axis is logarithmically spaced over a time interval ranging from 100 ns to 60 s. In this mode the correlator uses 216 time channels. The samples were dissolved in deionized water (Milli-Q purification system, 0.056 μS conductivity) at concentrations ranging from 1 mg l^{-1} to 300 g l^{-1} . The solutions were cleared of dust particles by filtering 3–10 times through a Millipore GS 0.2 μm pore-size filter.

In dynamic light scattering experiments, the time autocorrelation function of the scattered intensity $g_2(t)$ was measured (homodyne method), which was converted to the scattered electric field autocorrelation function $g_1(t)$ via the Siegert relation³⁶:

$$g_1(t) = \{[g_2(t) - A]/A\}^{1/2}$$

where A is the experimentally determined baseline.

The reduced scattering intensities Kc/R_θ were calculated according to standard procedures using toluene as the reference with known absolute scattering intensity. The volume-corrected scattering intensities of toluene varied by less than $\pm 1\%$ in the angular range from 30° to 150° , demonstrating the excellent calibration of the instrument.

Data analysis

The experimental correlation function $g_1(t)$ was fitted to a sum of exponentials using a SIMPLEX algorithm. If two well separated relaxations were observed, the following fitting procedure was applied, which is demonstrated for the sample P1Q2 at 30 g l^{-1} in salt-free solution at a scattering angle $\vartheta = 90^\circ$.

First, the slow relaxation is fitted to a sum of two exponentials (Figure 1):

$$g_1^{\text{slow}}(t) = a_1(q) \exp[-t/\tau_1(q)] + a_2(q) \exp[-t/\tau_2(q)]$$

The remaining fast relaxation is fitted by one exponential (Figure 2):

$$g_1^{\text{fast}}(t) = a_3(q) \exp(-t/\tau_3)$$

The final residues (Figure 3) show some systematic deviations, which are smaller than 0.3% and are considered to be insignificant for the purposes of the present work. For the slow and fast relaxation processes, the first cumulant Γ_1 is calculated according to:

$$\Gamma_1^{\text{slow}}(q) = \frac{1}{a_1 + a_2} \left(\frac{a_1(q)}{\tau_1(q)} + \frac{a_2(q)}{\tau_2(q)} \right)$$

$$\Gamma_1^{\text{fast}}(q) = \frac{1}{\tau_3(q)}$$

The apparent diffusion coefficients corresponding to the fast and the slow processes are evaluated as:

$$D_f(q) = \Gamma_1^{\text{fast}}(q)/q^2$$

and

$$D_s(q) = \Gamma_1^{\text{slow}}(q)/q^2$$

respectively. Here q is the scattering vector defined by $q = (4\pi n_0/\lambda_0) \sin(\vartheta/2)$ with n_0 the refractive index of the medium and λ_0 the wavelength of the incident light *in vacuo*.

If only one relaxation is present, the correlation function is fitted by either one or two exponentials and the first cumulant is calculated as described above.

RESULTS

Static scattering in salt-free solutions

Upon dilution, polyelectrolytes in aqueous, salt-free

solution exhibit quite an unusual behaviour. The static light scattering experiments demonstrate that the scattered intensity $I(q)$ does not show simple c and q dependences. In Figure 4 the reduced scattering intensity $I(0)/I(q)$ is plotted versus q^2 for six different concentrations ranging from 0.03 to 30 g l^{-1} . We here refer to $I(0)/I(q)$ rather than to the reduced scattering intensity $kc/R(q)$, which is usually discussed. The absolute value of $kc/R(q)$ for polyelectrolyte solutions is a rather complex quantity and its interpretation is beyond the scope of this publication.

Only for the highest concentrations is $I(0)/I(q)$ proportional to q^2 as expected for flexible, linear macromolecules. An apparent radius of gyration $R_{g,\text{app}}$, evaluated at a concentration of 100 g l^{-1} , is determined from the initial slope to be 460 Å for P4Q1, 690 Å for P1Q2 and 920 Å for P5Q1. The subscript 'app' denotes the missing extrapolation to zero concentration. $R_{g,\text{app}}$ increases with increasing molecular weight and charge density. The $R_{g,\text{app}}$ values of the quaternized polymers are much larger than those of the corresponding unquaternized poly(2-vinylpyridine) samples. For the smallest molecular weight, $R_{g,\text{app}}$ is even higher than calculated for a single rigid rod structure. It is therefore unlikely that the measured $R_{g,\text{app}}$ corresponds to the size of separated single macromolecules.

At lower concentrations the slope of $I(0)/I(q)$ vs. q^2

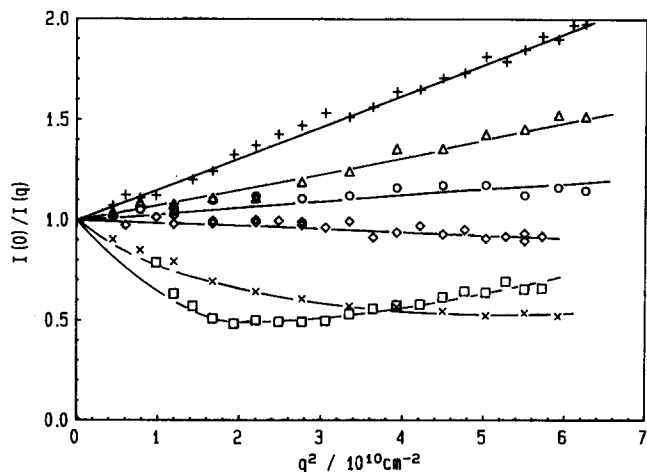


Figure 4 The reciprocal, normalized scattering intensity $I(0)/I(q)$ plotted versus the scattering vector q^2 for different salt concentrations: (+) 30, (Δ) 5, (\circ) 1, (\diamond) 0.3, (\times) 0.1, (\square) 0.03 g l^{-1} (sample P1Q2)

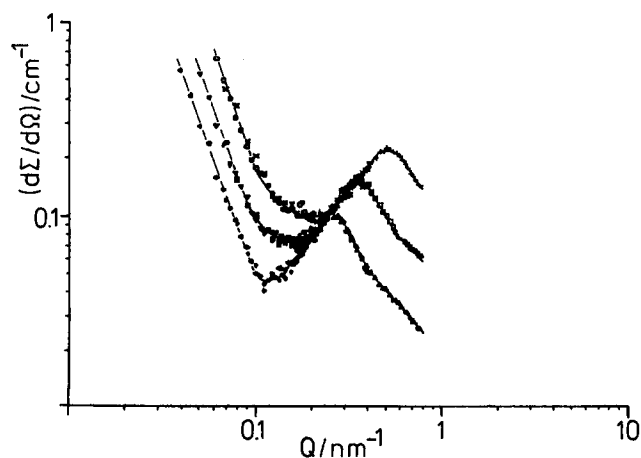


Figure 5 The differential cross section $d\Sigma/d\Omega$ plotted versus the scattering vector q . The upper curve corresponds to $c_{pe} = 25 \text{ g l}^{-1}$, the middle curve to 10 g l^{-1} and the lower curve to 5 g l^{-1} (sample P1Q2)

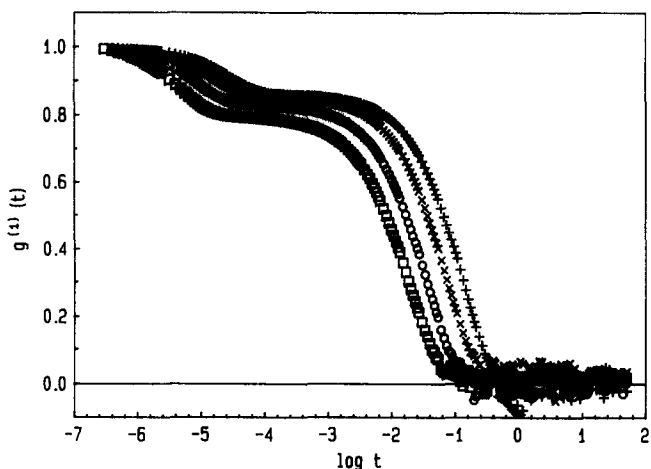


Figure 6 Correlation functions recorded at four different angles as functions of the time t , where t is in units of seconds: (+) 45°, (x) 60°, (O) 90°, (□) 140° (sample P1Q2)

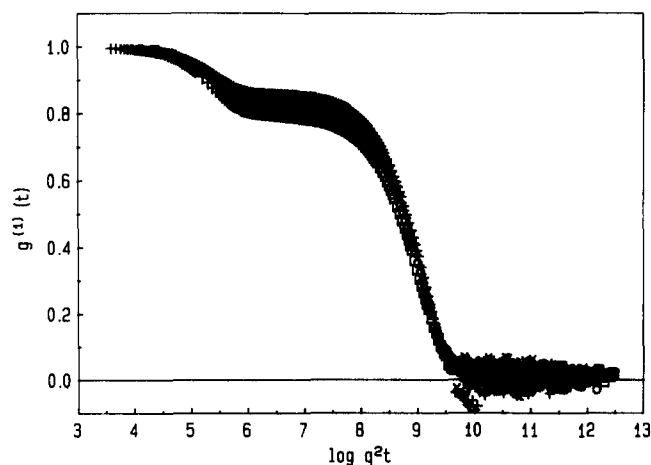


Figure 7 The same functions as in Figure 6, plotted versus $q^2 t$

becomes negative. At a concentration of 0.03 g l^{-1} , a minimum is observable at a value of q corresponding to the maximum scattered intensity.

For concentrations $c_{pe} \geq 1 \text{ g l}^{-1}$, the polyelectrolyte solutions were also investigated by small-angle neutron scattering³⁷. In Figure 5 the scattered intensity is plotted versus q for three different concentrations ranging from 5 to 25 g l^{-1} . The scattering curves exhibit three characteristic regimes. At low values of q , a sharp decrease in the scattering intensity with increasing q is observed, which approximately follows a power law $I(q) \sim q^{-a}$ with exponent $a \approx 2.7$. In the intermediate q regime we find a broad peak, the position of which changes with concentration. The shape and size of the peak are not affected by changes in polyelectrolyte concentration. At high values of q , $I(q)$ is proportional to q , i.e. a plateau value is reached if $qI(q)$ is plotted versus q . From the absolute scattered intensity of this plateau (Holtzer asymptote) the molecular mass per unit chain length is calculated as approximately 200 g mol^{-1} per monomer unit, which is in reasonable agreement with the theoretical value of 233 g mol^{-1} expected for a fully elongated chain conformation.

Dynamic scattering in salt-free solution

For the subsequent discussion the amplitudes of all autocorrelation functions $g_1(t)$ are normalized to unity.

The actual amplitudes lie between 0.15 for the lowest and 0.8 for the highest concentrations.

The q dependence at high concentrations. The correlation functions in Figure 6 are representative of measurements at high concentrations ($c_{pe} > 0.1 \text{ g l}^{-1}$) and show two well separated relaxation times at all scattering angles ϑ . The relative amplitude of the fast relaxation increases with increasing ϑ . If plotted against $q^2 t$ (Figure 7) it is seen that both relaxation times scale with q^2 as is expected for diffusive processes. From the correlation functions, the corresponding diffusion coefficients and the relative amplitudes can be calculated according to the procedure described in the 'Experimental' section. The diffusion coefficients of the fast process, D_f , and of the slow process, D_s , are plotted versus q^2 in Figure 8. Clearly, D_f is almost independent of q whereas D_s exhibits a pronounced q dependence.

The q dependence at low concentrations. Valuable information is extracted from a narrow concentration range around 0.1 g l^{-1} where two relaxations are observed together with an intermolecular structure factor in the static scattering intensity. As demonstrated in Figure 9, D_s is still increasing with increasing q . Also D_f exhibits an unusual negative slope as a function of q . This is regarded as direct evidence for the presence of strong intermolecular correlations.

At even lower concentrations ($c_{pe} < 0.1 \text{ g l}^{-1}$) only one broad relaxation mode is observed. The relaxation time

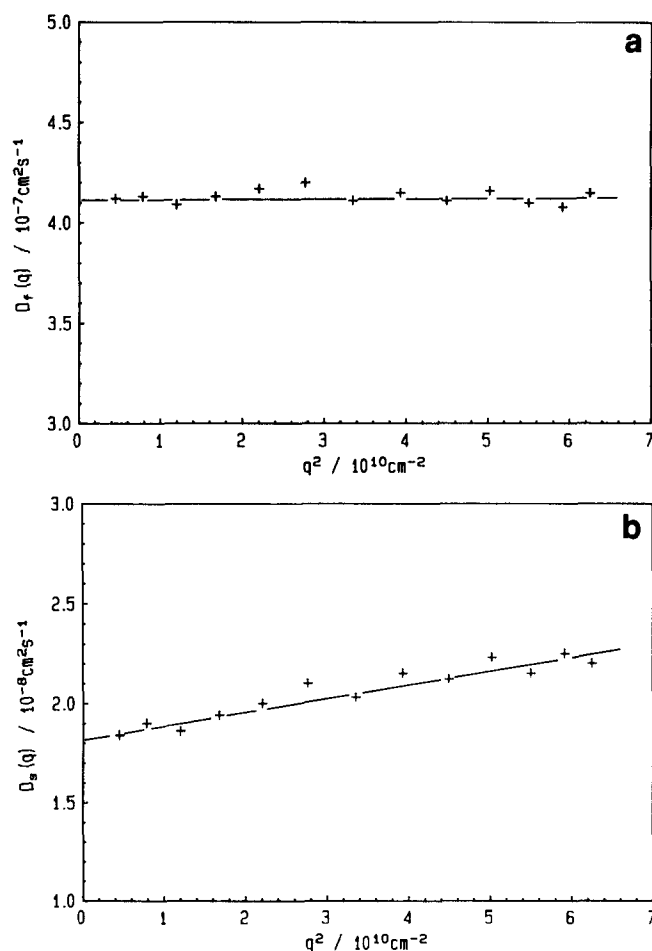


Figure 8 The diffusion coefficients (a) D_f and (b) D_s plotted versus q^2 for the sample P1Q2 ($L_w = 8300 \text{ \AA}$) at 30 g l^{-1}

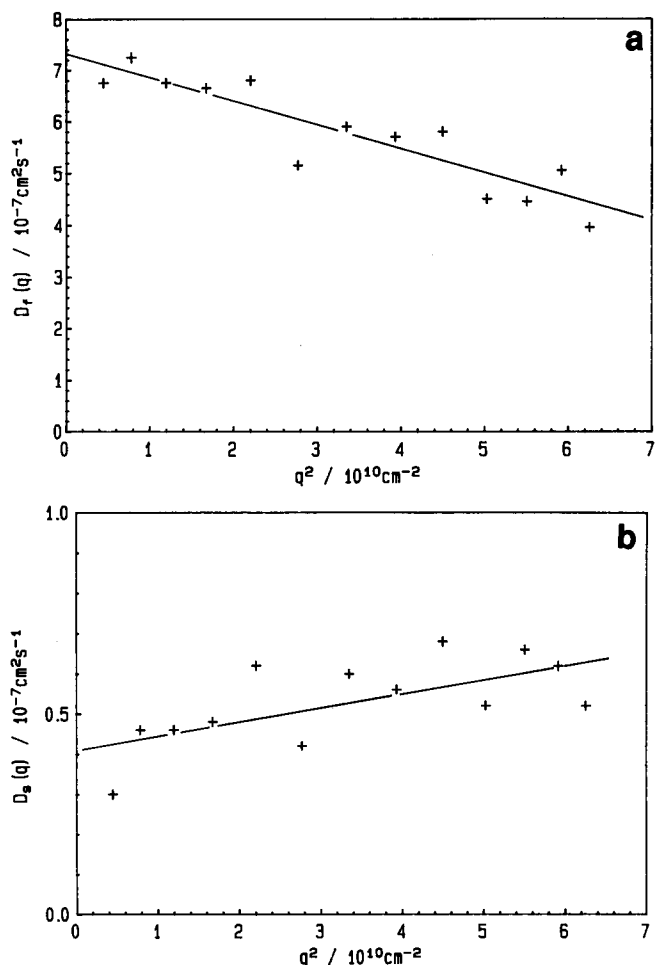


Figure 9 The diffusion coefficients (a) D_f and (b) D_s plotted versus q^2 for the sample P1Q2 ($L_w = 8300 \text{ \AA}$) at 0.1 g l^{-1}

does not show a simple q dependence, as demonstrated in Figure 10. The corresponding diffusion coefficient exhibits a negative slope when plotted against q^2 . This indicates that even at the lowest measured concentrations the polyelectrolyte system exhibits strong intermolecular interactions.

Concentration dependence. In Figure 11 the concentration dependence of the correlation functions $g_1(t)$ recorded at 90° for P4Q1 are shown. It is qualitatively observed that the relaxation time of the fast decay remains almost concentration-independent, whereas the relaxation time of the slow process decreases with increasing concentration. The relative amplitude of the slow relaxation decreases with decreasing concentration and eventually disappears completely.

Figure 12 shows the values of the diffusion coefficients extrapolated to zero angle as functions of the polyelectrolyte concentration, c_{pe} , for five different polyelectrolytes. Three different concentration regimes can be distinguished. At very low concentrations ($c_{pe} < 0.01 \text{ g l}^{-1}$, dilute lattice regime) we observe one diffusive process only, which is independent of concentration and only slightly dependent on molecular weight. For $0.01 \leq c_{pe} \leq 0.1 \text{ g l}^{-1}$ there is a transition regime, where D increases to D_f and a slow process, characterized by D_s , gradually appears. Changes in molecular weight do not significantly affect the location of the transition regime. In the third regime ($c_{pe} > 0.1 \text{ g l}^{-1}$, semidilute lattice regime), D_f is independent of c_{pe} and molecular weight. D_s is found to

decrease with increasing concentration and molecular weight. As seen from the behaviour of P1Q1 and P1Q2, the charge density does not significantly affect the diffusive behaviour. For very high concentrations ($c > 100 \text{ g l}^{-1}$) all relaxation processes are slowed down due to the strongly increasing local friction.

Static light scattering with added salt

Figure 13 shows the reduced scattering intensity $I(0)/I(q)$ for P1Q2 at constant polymer concentration, $c_{pe} = 0.33 \text{ g l}^{-1}$, but varying salt concentration. As the salt concentration increases, the influence of the intermolecular structure factor becomes less pronounced, as indicated by the drastic change of the initial slope from negative to positive values. For 0.01 mol l^{-1} salt, a maximum slope is reached, which decreases slightly upon further addition of salt. This decrease of $R_{g,app}$ is qualitative evidence of a coil contraction with increasing ionic strength. For a salt concentration of 0.1 mol l^{-1} $R_{g,app}$ is only slightly higher than $R_g = 220 \text{ \AA}$, measured for the unquaternized sample in THF³².

Dynamic light scattering with added salt

Dynamic light scattering was performed simultaneously with the static light scattering experiments described in

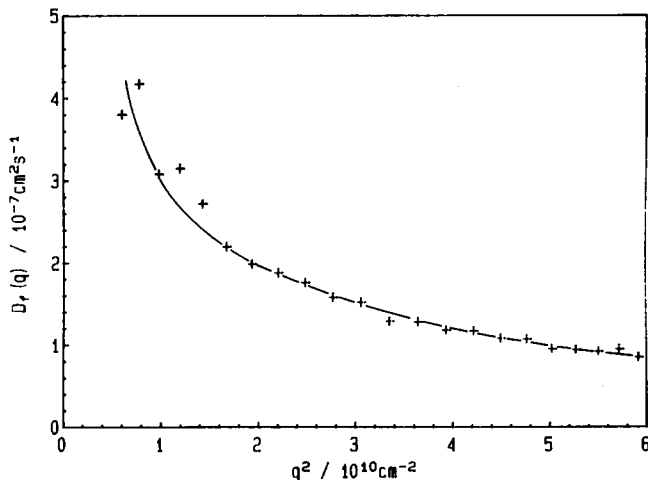


Figure 10 The diffusion coefficient D_f plotted versus q^2 for the sample P1Q2 ($L_w = 8300 \text{ \AA}$) at 0.04 g l^{-1}

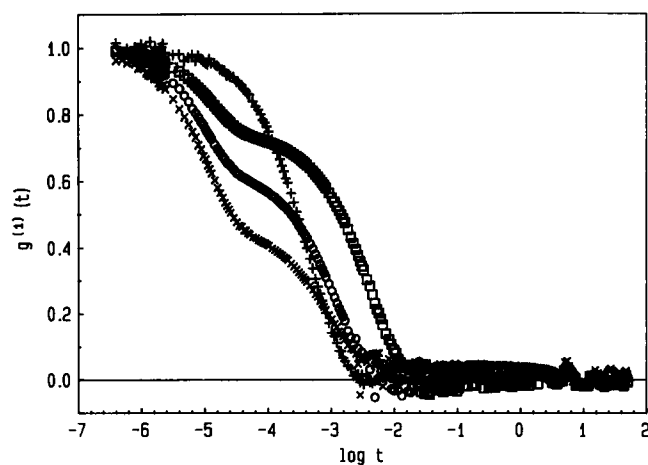


Figure 11 Concentration dependence of the correlation functions for the sample P4Q1 ($L_w = 1300 \text{ \AA}$): (\square) 100, (\circ) 5, (\times) 1, ($+$) 0.01 g l^{-1}

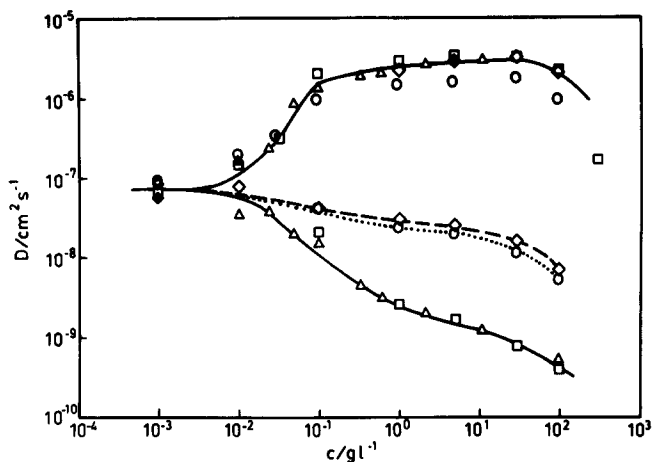


Figure 12 The diffusion coefficients extrapolated to zero angle as a function of polyelectrolyte concentration, c_{pe} (g l^{-1}): (\square) P1Q2 ($M_w = 780\,000 \text{ g mol}^{-1}$, $Q = 75\%$); (\triangle) P1Q1 ($M_w = 580\,000 \text{ g mol}^{-1}$, $Q = 40\%$, data taken from ref. 16); (\diamond) P4Q1 ($M_w = 109\,000 \text{ g mol}^{-1}$, $Q = 65\%$); (\circ) P3Q3 ($M_w = 200\,000 \text{ g mol}^{-1}$, $Q = 98\%$); (\blacklozenge) P5Q1 ($M_w = 2\,260\,000 \text{ g mol}^{-1}$, $Q = 100\%$)

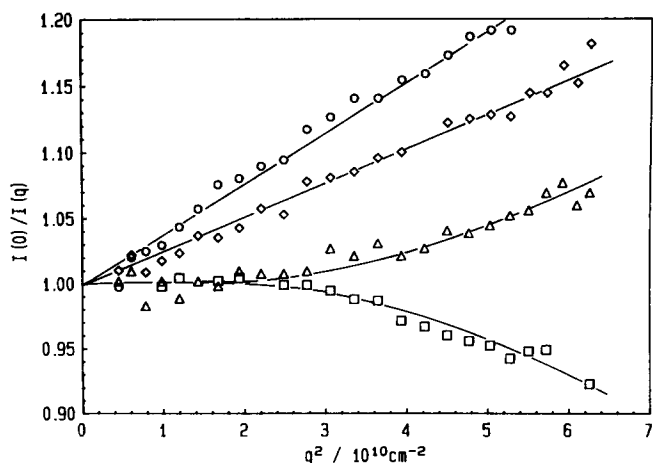


Figure 13 The reciprocal, normalized scattering intensity $I(0)/I(q)$ plotted versus the scattering vector q^2 for different salt concentrations at constant polyelectrolyte concentration of 0.33 g l^{-1} (sample P1Q2, $L_w = 8300 \text{ \AA}$): (\diamond) 0.1, (\circ) 0.01, (\triangle) 0.003, (\square) 0.001 mol l^{-1}

the foregoing subsection. At high salt concentration ($c_s > 10^{-3} \text{ mol l}^{-1}$), only one relaxation mode is apparent. At $c_s = 0.001 \text{ mol l}^{-1}$, a weak (i.e. small-amplitude) slow relaxation becomes observable, and the relaxation time of the fast mode increases (Figure 14). For salt-free solutions two well separated relaxation processes are detected, corresponding to the results shown in Figure 6. In Figure 15, the values of the diffusion coefficients, extrapolated to zero angle, are plotted versus the salt concentration c_s . As for salt-free solutions a classification into three concentration regimes is feasible. At high salt concentration ($c_s \geq 0.01 \text{ mol l}^{-1}$) the relaxation mode is independent of c_s . Between 0.003 and $0.0001 \text{ mol l}^{-1}$ a transition occurs, where D increases to D_f , and a slow diffusion becomes observable. For concentrations $c_s \leq 0.0001 \text{ mol l}^{-1}$, both diffusion coefficients are nearly independent of the salt concentration. This dynamic behaviour is equivalent to the 'ordinary-extraordinary transition'²². The present results demonstrate that the dynamic changes described should not be referred to as a 'transition', but rather as an 'onset of splitting', where a slow diffusion gradually appears.

In order to check whether or not the 'onset of splitting' depends on the absolute ionic strength of the solution, the polymer concentration was varied at constant added salt concentrations ($0.001 \leq c_s \leq 0.1 \text{ mol l}^{-1}$). The results are displayed in Figure 16a, where the diffusion coefficients, extrapolated to zero angle, are plotted versus the polyelectrolyte concentration for different salt concentrations. The polymer concentration at which the splitting starts is strongly dependent on the concentration of added salt. If c_s is increased by one order of magnitude, the transition regime is shifted to higher c_{pe} by approximately one order of magnitude as well. This is demonstrated in Figure 16b, where the results shown in Figure 16a are now plotted versus the ratio λ , where λ is the molar ratio of the polyion charges to the added salt. A remarkably good superposition of the curves is obtained, which proves the negligible influence of the absolute ionic strength on the dynamic behaviour of polyelectrolytes. Since for the salt-free solutions the 'salt' concentration is not known, we varied c_s until reasonable superposition with the other curves was achieved. This procedure yielded $c_s = 6 \times 10^{-5} \text{ mol l}^{-1}$ for the 'salt-free' solution, which lies within the expected range.

DISCUSSION

Static scattering

Most theoretical treatments of polyelectrolyte solution structure consider the influences of both intrachain and interchain correlations. These can be readily expressed in terms of the total scattering function $I(q)$, which is defined as:

$$I(q) = \sum_{\alpha} \sum_{\beta} \sum_i \sum_j a \exp[-iq(r_{\alpha i} - r_{\beta j})]$$

where q is the scattering vector, a is the scattering length of a monomer, α and β indicate different chains, and i and j are the monomers within the chains α and β . If the two contributions from intrachain correlations ($\alpha = \beta$) and interchain correlations ($\alpha \neq \beta$) can be separated, $I(q)$ may be written as:

$$I(q) = S(q)P(q)$$

where the form factor $P(q)$ corresponds to intrachain correlations and $S(q)$ corresponds to interchain correlations.

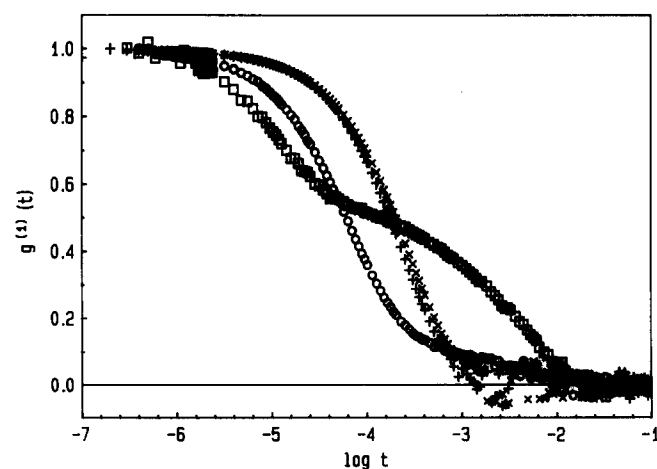


Figure 14 Correlation functions recorded at $\theta = 90^\circ$ for P1Q2 (0.03 g l^{-1} , $L_w = 8300 \text{ \AA}$) at different salt concentrations: (+) 0.1, (x) 0.01, (o) 0.001 mol l^{-1} , (\square) 'salt-free'

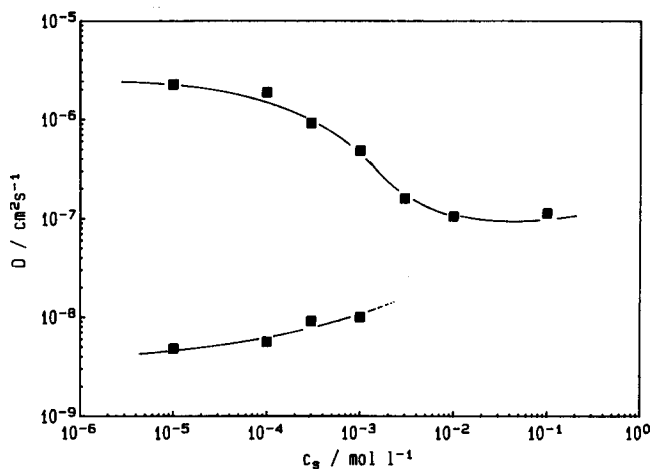


Figure 15 The diffusion coefficients, extrapolated to zero angle, plotted versus salt concentration, c_s (mol l^{-1})

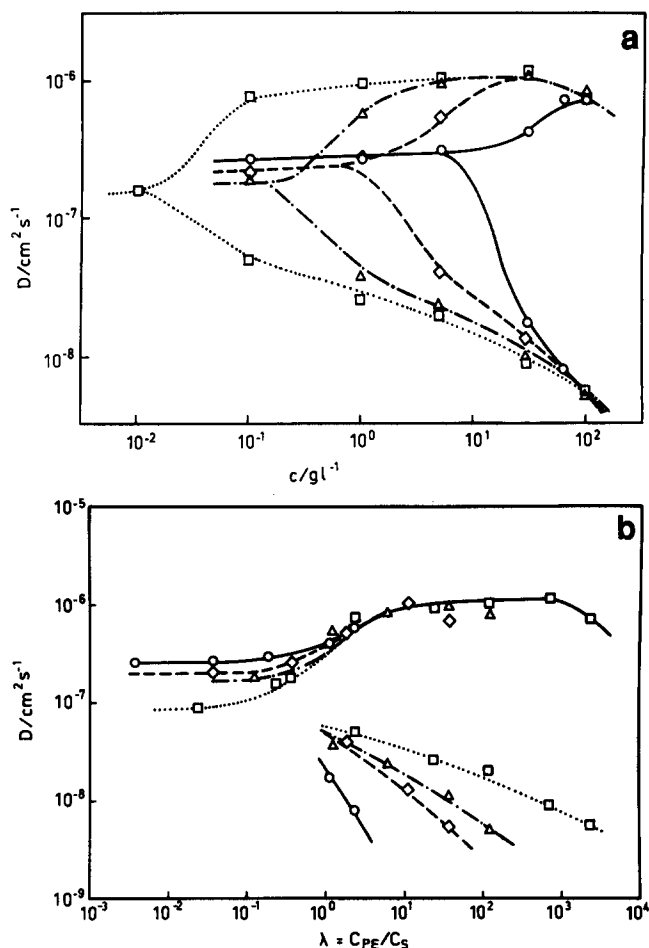


Figure 16 (a) The diffusion coefficients, extrapolated to zero angle, plotted versus polyelectrolyte concentration c_{pe} (g l^{-1}) for the sample P3Q3 ($L_w = 1800 \text{ \AA}$) for different salt concentrations, c_s : (\square) 'salt-free', (\triangle) 10^{-3} , (\diamond) 10^{-2} , (\circ) $10^{-1} \text{ mol l}^{-1}$. (b) The same diffusion coefficients, plotted versus $\lambda = c_{pe}/c_s$: (\square) 'salt-free', (\triangle) 10^{-3} , (\diamond) 10^{-2} , (\circ) $10^{-1} \text{ mol l}^{-1}$

The observation of a peak in the scattering function $I(q)$ seems to be a characteristic feature of polyelectrolyte solutions without added salt. This peak in the scattering curve has been interpreted either in terms of a correlation hole^{38,39} or in terms of the presence of an ordered structure in the solution^{2,3,6,8}.

The idea of a correlation hole was first introduced by de Gennes⁴⁰. In this model, each polyelectrolyte chain is surrounded by a correlation tube from which other chains are strongly expelled. The radius of the tube is equal to the screening length κ^{-1} . The intermolecular structure factor $S(q)$ of the correlation hole has been suggested by Hayter *et al.*³⁸ to be:

$$S(q) = \frac{q^2 \xi^2}{1 + q^2 \xi^2}$$

where ξ is interpreted as the average distance between neighbouring chains. A different expression has been proposed by Koyama³⁹:

$$S(q) = 1 - \exp(-\kappa^2 q^2 / 4)$$

Both are continuously increasing functions of q , which reach the asymptotic value of 1 at high q . If $P(q)$ is taken as the form factor of a rigid rod, $I(q)$ exhibits a maximum at $q_m = \xi^{-1}$, corresponding to the experimental results. However, in recent SANS studies Nierlich *et al.*²⁰ showed that $S(q)$ solely exhibits a maximum, which disproves the correlation hole argument.

The idea that polyelectrolytes may form ordered structures has been adopted by several theoretical approaches. As an example, we would like to discuss the model of de Gennes *et al.*³ in some detail.

At very low concentrations (*dilute regime*) different polyion chains are not overlapping and are very far from each other. The overall size of the polyion is proportional to the degree of polymerization. There is a range of slightly higher concentrations c_{pe} ($c^{**} < c_{pe} < c^*$) where chains do not overlap ($c < c^*$) but where the electrostatic interactions between polyions are much larger than thermal energies ($c > c^{**}$). Here it is expected that the polyions build up a three-dimensional periodic lattice (*dilute lattice regime*). At concentrations $c > c^*$ (*semidilute regime*) different chains overlap with each other. De Gennes *et al.* considered several possible conformations: (a) a hexagonal lattice of rigid rods, (b) a cubic lattice of rigid rods, and (c) an isotropic phase of partially flexible chains. It was suggested that case (c) is the more probable structure. In the *isotropic model* each chain

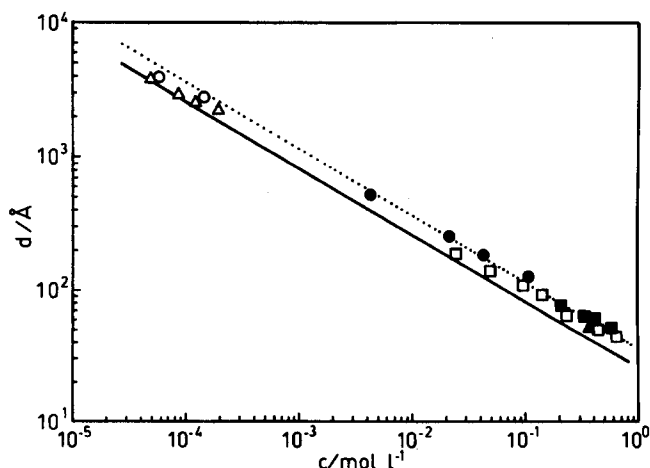


Figure 17 Experimentally determined intermolecular distances d (\AA) plotted versus the polyelectrolyte concentration c_{pe} (mol l^{-1}): (\triangle) ref. 13, (\circ) ref. 16, (\bullet) ref. 37, (\square) ref. 19, (\blacksquare) ref. 20, (\blacktriangle) ref. 21. The full line is calculated according to $d = (1/acN_A)^{1/2}$, where a is the monomer length (2.5 \AA), c is the polyelectrolyte concentration (mol l^{-1}) and N_A is Avogadro's number. For the dotted line $d = (2/acN_A)^{1/2}$

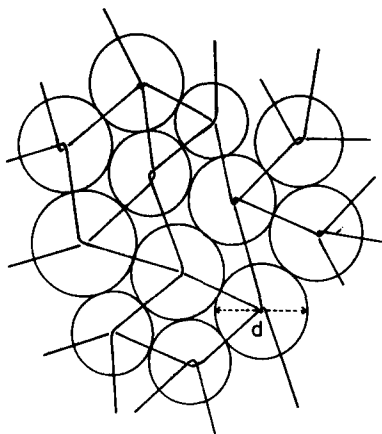


Figure 18 Model of a transient network of polyelectrolytes

consists of a random succession of segments of size 1. Within one segment the electrostatic effect dominates and gives rise to the elongated conformation of the segment. Between different segments the interactions are screened. For chains consisting of many segments an ideal chain behaviour results, characterized by $R_g(c) \sim c^{-1/4} N^{1/2}$. If it is assumed that the dynamic effects of entanglements are weak compared with the electrostatic contribution, this leads to a viscosity $\eta_{sp}/c = Nc^{-1/2}$ (Fuoss law⁴¹).

If the scattering intensity exhibits a maximum at the scattering vector q_m , then the intersegmental distance is $d = 2\pi/q_m$ according to Bragg's law. In Figure 17 the experimental distances d , taken from several recent publications including our own results, are plotted versus the concentration. The full line corresponds to a two-dimensional close packing of rigid cylinders of length $L = aN$. Except for very low c_{pe} , the experimental points lie significantly above this curve. Nierlich *et al.*²⁰ realized this discrepancy and introduced some chain flexibility, which reduces the cylinder length to $L = \langle R^2 \rangle^{1/2}$, with $\langle R^2 \rangle^{1/2}$ the end-to-end distance of a Kratky-Porod worm-like chain. Although this picture may satisfactorily describe the static neutron scattering results, it encounters serious problems in describing the dynamic behaviour of the system, as will be demonstrated later.

Here we wish to discuss the isotropic entangled network of de Gennes *et al.*³. In this model the entangled system is visualized as a three-dimensional close packing of spheres of diameter d (Figure 18). One sphere contains on average one entanglement of two different chains, which randomly connect the nearest-neighbour spheres. The point is that a doubled mass density of chains on the lattice occurs, because two chains are present within one 'entanglement blob', i.e. the spherical subunit on the lattice. In Figure 17 this model is represented by the upper dotted line, which at high concentrations describes the experimental data satisfactorily. At very low c , the entangled network must fall apart and the concept of ordered cylinders may be more appropriate.

Only little is known of how added salt influences the height and position of the peak. One more or less incomplete study¹⁹ reveals that addition of salt at fixed polyelectrolyte concentration diminishes the peak height, but does not significantly alter the maximum q value, q_m . The current explanation is that the addition of salt screens the electrostatic interactions and eventually destroys the intermolecular structure.

Dynamic scattering

Our results suggest that the concentration dependence of the diffusion is characterized by three different concentration regimes. These regimes are mainly determined by the ratio of polymer and salt concentrations, $\lambda = c_{pe}/c_s$, but not by the absolute ionic strength of the solution.

In the dilute lattice regime ($\lambda \ll 1$) only one diffusive process is observed, which at very low ionic strength is hardly influenced by the molecular weight of the polyelectrolyte. This indicates that at low salt and low polymer concentration the electrostatic interaction determines the diffusion rather than the hydrodynamic friction of the molecules. However, it is well known that at high ionic strength, i.e. high salt and low polymer concentration, the polyelectrolytes behave essentially like neutral polymers in dilute solutions. Thus, in this regime an $M^{-\nu}$ ($0.5 \leq \nu \leq 0.6$) dependence of the diffusion coefficient is expected, where M is the molecular weight of the polyelectrolyte. We believe that with increasing salt concentration the molecular-weight dependence of D gradually becomes more pronounced until the behaviour expected for neutral polymers is reached. Experiments to test this explanation are currently in progress. For the present example D increases only slightly with increasing c_s . This behaviour is consistent with the possibility that the hydrodynamic diffusion at high salt is only slightly larger than the 'electrostatic' diffusion at low salt concentration.

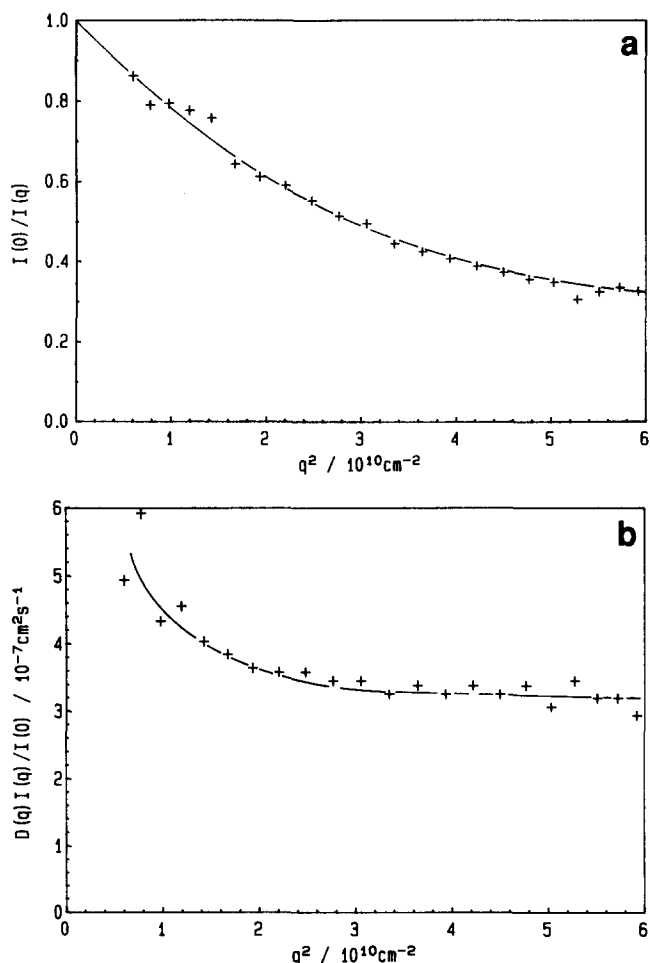


Figure 19 The reciprocal, normalized scattering intensity $I(0)/I(q)$ and the quantity $D(q)I(q)/I(0)$ plotted versus the scattering vector q^2 for P1Q2 ($L_w = 8300 \text{ \AA}$) at 0.04 g l^{-1}

Spatial ordering has pronounced effects on the dynamics of the polyelectrolyte chains. If the solution is probed on length scales of the order of the typical intermolecular distance, where the scattered intensity is strongly influenced by the intermolecular structure factor $S(q)$, the cooperative diffusion coefficient D is also a function of $S(q)$ and the classical relation:

$$D(q) = \frac{D_0}{S(q)P(q)}$$

approximately holds, with D_0 the free-draining particle diffusion coefficient (without hydrodynamic interaction). This was first proposed by Ackerson⁴² and by Hess and Klein¹⁰.

Our static and dynamic light scattering experiments show that the *fast diffusion*, observed in the transition regime, is strongly influenced by the intermolecular structure factor as demonstrated by the q dependence of $D_f(q)$ (Figure 10), $I(0)/I(q)$ (Figure 19a) and $D_f(q)I(q)/I(0)$ (Figure 19b). For large values of q , the quantity $D_f(q)I(q)/I(0)$ is found to be q -independent. Qualitatively similar results were obtained by Drifford and Dalbiez¹³, who investigated dilute NaPSS solutions by light scattering, and by Kaji *et al.*⁸, who applied the Neutron Spin Echo (NSE) technique for NaPSS at higher concentrations. A closer inspection of our results reveals that $D_f(q)I(q)/I(0)$ seems to diverge at small q values. If the first cumulant Γ_1 is plotted *versus* q^2 (Figure 20), a straight line with a non-zero intercept is obtained. The intercept corresponds to a q -independent relaxation. Such a behaviour was theoretically predicted by Akcasu *et al.*⁹, who calculated the dynamics of point-like charged molecules in solution under the influence of hydrodynamic interactions by means of the projection operator technique. In the limit of $q \rightarrow 0$ they obtain:

$$\Gamma_1 = D_1\kappa_1^2 + D_2\kappa_2^2 + \frac{kT}{\pi\eta_0} \frac{\kappa_1^2\kappa_2^2}{3\kappa}$$

with D_1 the diffusion coefficient of the monomer, D_2 the diffusion coefficient of the counterion, κ^{-1} the Debye screening length with $\kappa^2 = \kappa_1^2 + \kappa_2^2$, and the last term of the equation being due to hydrodynamic interactions. The constant relaxation frequency at $q=0$ is referred to as the 'plasmon mode', in analogy with the total plasma frequency. In our case, the relaxation time is of the order of 0.5 ms. To our knowledge this is the first experimental evidence to support this concept for polyelectrolyte solutions.

The results outlined above indicate further that the fast diffusive process, which is observed in the transition regime and in the semidilute regime, takes place within an ordered structure, i.e. an at least partially ordered dilute lattice with a correlation length d .

In the *semidilute regime*, where $\lambda \gg 1$, we observe both a fast and a slow diffusive process. The coefficient of the fast diffusion D_f is independent of λ and of the molecular weight. D_s , corresponding to the slow process, decreases slightly with increasing λ and also with increasing molecular weight.

At very high polyelectrolyte concentrations ($c_{pe} > 100 \text{ g l}^{-1}$), the values of the diffusion coefficients decrease strongly with increasing c_{pe} , which is due to strongly increasing local friction in these highly viscous solutions.

A fast concentration-independent diffusion was also found by other groups^{12,14,15} and was attributed to

cooperative fluctuations in polymer concentration. It was suggested^{13,15} that the fast diffusion represents the Nernst–Hartley diffusion of polyions. We observe the fast diffusion up to very high concentrations of 300 g l^{-1} for a polyelectrolyte of molar mass $750\,000 \text{ g mol}^{-1}$. This is well above the overlap concentration where it is unlikely that Nernst–Hartley diffusion of single polyions takes place. Alternatively, the fast mode may result from thermally excited displacement fluctuations of polymer segments between entanglements. This is usually referred to as the gel mode of a transient network. Since the gel mode is a local property of the polyelectrolyte, it is independent of molecular weight, in agreement with the experimental results. The existence of a gel mode and the observation that the gel mode occurs in an ordered structure is compatible with the model discussed in Figure 18. It is interesting to note that recent static and dynamic light scattering studies on swollen, permanently cross-linked poly(acrylic acid) networks⁴³ show qualitatively the same dynamic behaviour. These authors postulate that fluctuations in a swollen polyelectrolyte network are dominated by the osmotic pressure of the counterions. This interpretation may also be feasible for our case of transient networks of linear polyelectrolytes.

At this point we wish to return to the discussion concerning the origin of the peak in the static neutron scattering curves. We do not see any possibility of how a two-dimensional close packing of semi-flexible segments, as suggested by Nierlich *et al.*²⁰, could simultaneously exhibit both fast and slow diffusive modes.

The *slow diffusion*, which is observed in both the transition regime and in the semidilute regime, has been attributed either to reptation¹⁴ or to a diffusion process of interchain domains (clusters) having relatively large dimensions^{15,16}. According to the reptation model $D \sim M^{-2}c^{-3}$. In our case the exponent of the molecular-weight dependence of D_s depends strongly on the concentration and eventually a small regime is reached where $D \sim M^{-2}$ is experimentally observed. Much clearer experimental evidence against the reptation picture is given by the concentration dependence of D_s , the exponents of which vary for the different investigated molecular weights and concentrations between -0.1 and -1 .

As shown in Figures 8 and 9, a q dependence of D_s is observed, which can be explained by the polydispersity in size of the diffusing objects or by internal modes of motion of usually quite large structures. Together with

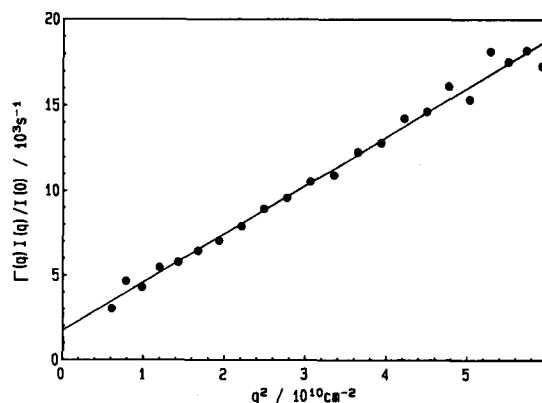


Figure 20 The relaxation time Γ plotted *versus* q^2 for P1Q2 ($L_w = 8300 \text{ \AA}$) at 0.04 g l^{-1}

the angular dependence of D_s , we observe a pronounced q dependence of $I(q)$. From the initial slope of $I(q)$ as a function of q^2 , $R_{g,app}$ values between 400 and 1000 Å are evaluated. At constant polyelectrolyte concentration, $R_{g,app}$ increases with increasing molecular weight, which parallels the observation that D_s decreases with increasing molecular weight. Also, D_s decreases with increasing polyelectrolyte while $R_{g,app}$ increases. Obviously, D_s and $R_{g,app}$ are strongly related and indicate that the slow diffusion is caused by the motion of large domains. This is also supported by the results of Sedlak *et al.*¹⁵ in a study of the dynamics of poly(acrylic acid).

The nature of the domains is not yet completely elucidated. Our static light scattering experiments demonstrate that the domains exhibit a definite size as characterized by $R_{g,app}$. Additional information results from our small-angle neutron scattering studies. For small values of q a power-law behaviour $I(q) \sim q^{-a}$ is observed, the exponent of which may be related to the fractal dimension of the particle. We find a value of $a = 2.7$, which is close to 2.5, a value typical for diffusion-limited cluster aggregation⁴⁴.

The origin of the slow diffusion coefficient was frequently discussed in the literature, particularly in the context of the so-called 'ordinary-extraordinary' transition, which will be discussed below in more detail. In the context of the isotropic entangled network model developed for static scattering, we here speculatively attribute the slow diffusion process to long-range concentration fluctuations of large domains, which are randomly created at random places in the network. Consequently these fluctuations exhibit no order and may diffuse freely. These long-range instabilities may originate from the delicate electrostatic balance between both polyions and low-molecular-weight ions, involved in this physical network, which may be easily disturbed by fluctuation of the thermal energy. More experimental evidence of the nature of D_s arises in the 'transition regime', which is discussed below.

At $\lambda \approx 1$ (*transition regime*), the value of the diffusion coefficient increases with increasing λ and the slow diffusive process gradually appears. This phenomenon is well described in the literature and referred to as an 'ordinary-extraordinary' transition²². The word 'transition' in this context may be misleading and in the following we shall term the change in behaviour the 'onset of splitting'. This onset of splitting is either achieved by changing the amount of salt at constant polyelectrolyte concentration or by variation of the polyelectrolyte content at constant salt concentration.

For the fast diffusion, scaling theory predicts $D \sim c_{pe}^{1/2}$ for salt-free solutions in the transition regime, which was experimentally verified by Grüner and Lehmann¹², and $D \sim c_{pe}^{3/4}$ for solutions with added salt which was experimentally observed by Koene *et al.*¹⁴. Our data suggest, however, that D increases sigmoidally from its value in the dilute regime to its plateau value in the semidilute regime, and no scaling relationship can be applied. It is qualitatively observed that the slope decreases with increasing salt. This is also supported by the experiments of Kurata *et al.*²³ on poly(L-lysine) at various polyelectrolyte and salt concentrations.

For the slow diffusion, no reasonable theoretical explanation exists as discussed above. Some remarks, however, should be made concerning the onset of splitting, which occurs at a constant ratio $\lambda^* = (1/k)(c_{pe}/c_s)$.

The proportionality constant k varies for different investigations and systems between 1.2 (this work) and 5 (Drifford and Dalbiez²⁸). The experimental value of k exhibits considerable scatter, because it depends strongly on the ability of the correlator to detect slow modes.

It should be pointed out that 'salt-free' solutions have a non-zero ion concentration caused by the dissociation of water. In our case, the quaternized nitrogen moieties of the polyelectrolyte and solubilized atmospheric CO₂ act as weak acids and increase the concentration of H⁺, characterized by the pH value of the solution. Experimentally determined pH values lie between 5.5 for dilute and 4.5 for concentrated polyelectrolyte solutions. The onset of splitting in 'salt-free' solution is observed at $c_{pe}/c_s \approx 1$ (with $c_s \approx 6 \times 10^{-5} \text{ mol l}^{-1}$), which in this respect indicates a universal behaviour of polyelectrolyte solutions independent of the absolute ionic strength.

Drifford and Dalbiez²⁸ give an empirical condition for the onset of splitting, given by the amount of salt necessary to destroy intermolecular ordering leading to another concentration regime:

$$\frac{c_{pe}}{\sum_i c_i Z_i^2} \frac{a}{Q} \approx Z_s$$

where $\sum_i c_i Z_i^2$ is the Debye screening due to added salt (species i , molarity c_i and valency Z_i), a is the distance between two successive charges on the polyion and Q is the Bjerrum length, the closest possible distance for two like charges in the solution at equilibrium. Q has a value of $7.1a$ at 25°C. Z_s is the valency of the counterion of the added salt.

The remaining discussion will be devoted to the nature of the slow diffusion. Particularly, poly(L-lysine) systems were carefully investigated by different experimental techniques in the vicinity of the onset of splitting. Slowly moving domains or particles as observed in dynamic light scattering experiments could not be detected in measurements of the self-diffusion coefficient by means of fluorescence bleaching recovery experiments²⁴ or in the electrophoretic mobility determined by electrophoretic light scattering²⁶. Schmitz and coworkers⁴⁵ found that rather weak electric fields effectively suppress the slow diffusion by destroying the large domains.

On the basis of these experiments Schmitz and Ramsay⁴⁵ suggested that temporal aggregates cause the slow diffusion. They developed the qualitative picture that at $\lambda < 1$ each polyion is surrounded by its own ion cloud. At $\lambda > 1$, the ion clouds of neighbouring polyions begin to overlap. The temporal aggregates are then stabilized by fluctuating forces arising from the small ions in the overlapping region, which are now shared by some neighbouring polyions. A similar model was proposed by Fulton^{46,47}. He examined phenomenological transport expressions for the relaxation of charge transport and demonstrated that long-range correlations between fluctuating dipoles persist over long periods of time. The importance of small-ion effects is also underlined by Drifford and Dalbiez²⁸ and by Kurata *et al.*²³. It may be pertinent in this context to recall the 'two-phase' model of Ise⁴⁸, who postulated the coexistence of disordered and ordered structures in polyelectrolyte solutions.

The picture of temporal aggregates is conceptually equivalent to our model of temporal domains in an ordered transient network. The stability of the fluctuating heterogeneities within the network is strongly dependent

on the number of low-molecular-weight ions between the polyions. These heterogeneities become unstable if every charge in the polyion is surrounded by one or more low-molecular-weight ions. In other words, the ions screen the electrostatic interaction of neighbouring segments in the network.

It should be noted that the long-range fluctuating heterogeneities within the network are not ordered, since D_s is not influenced by the intermolecular structure factor $S(q)$, as demonstrated in Figure 8. Particularly interesting are the results obtained in the region of splitting at low polymer and low salt concentrations, where we observed the plasmon mode according to the theory of Akcasu *et al.*⁹. In this regime, the postulated network heterogeneities and even the network itself become so unstable that the heterogeneities decay on a local scale with a short lifetime, i.e. no diffusive behaviour is observed but rather the local relaxation of heterogeneities.

CONCLUSIONS

We have unambiguously shown that the dynamic behaviour of polyelectrolyte solutions as measured by dynamic light scattering is dominated by the ratio of polyion to salt concentration, $\lambda = c_{pe}/c_s$, irrespective of the total ionic strength of the solution, the molecular weight of the polyion and the charge density. This observation is in qualitative agreement with other, less extensive, light scattering investigations and with recently published viscosity data on dilute polyelectrolyte solutions¹¹. The experimental results are qualitatively explained on the basis of the isotropic entangled network model as introduced by de Gennes *et al.* We currently believe that the occurrence of a structure peak in the static scattering intensity at high q values as measured by neutron scattering of semidilute solutions is also strongly related to the ratio $\lambda = c_{pe}/c_s$. Further SANS experiments to elucidate the effect of λ on solution structure are in progress. The absolute ionic strength of the solution, which is theoretically predicted to influence the chain stiffness of the polyelectrolyte, was found to be of minor importance, particularly in the semidilute regime. A pronounced effect of the ionic strength on the molecular-weight dependence of the diffusion coefficient at very dilute polyion concentrations and an understanding of this effect is the aim of our current investigations.

ACKNOWLEDGEMENT

We wish to thank Dr R. Borsali, MPI Mainz, for bringing ref. 9 to our attention. The support of the polymer analytical group at the MPI für Polymerforschung, Mainz, is gratefully acknowledged. We are indebted to Dr M. Aven for critical reading of the manuscript.

REFERENCES

- 1 For a review see Mandel, M. in 'Encyclopedia of Polymer Science and Engineering' (Eds. H. F. Mark, N. M. Bikales, C. G. Overberger and G. Menges), Wiley, New York, 2nd Edn., 1988, Vol. II, p. 739
- 2 Lifson, S. and Katchalsky, A. *J. Polym. Sci.* 1954, **13**, 43
- 3 De Gennes, P. G., Pincus, P., Velasco, R. M. and Brochard, F. *J. Physique* 1976, **37**, 1461
- 4 Odijk, T. *J. Polym. Sci., Polym. Phys. Edn.* 1977, **15**, 477
- 5 Skolnick, J. and Fixman, M. *Macromolecules* 1977, **10**, 944
- 6 Odijk, T. *Macromolecules* 1979, **12**, 688
- 7 Le Bret, M. *J. Chem. Phys.* 1982, **76**, 6243
- 8 Kaji, K., Urakawa, H., Kanaya, T. and Kitamaru, R. *J. Physique* 1988, **49**, 993
- 9 Akcasu, A. Z., Benmouna, M. and Hammouda, B. *J. Chem. Phys.* 1984, **80**, 2762
- 10 Hess, W. and Klein, R. *Adv. Phys.* 1983, **32**, 173
- 11 Cohen, J., Priel, Z. and Rabin, Y. *J. Chem. Phys.* 1988, **88**, 7111
- 12 Grüner, F., Lehmann, W. P., Fahlbusch, H. and Weber, R. *J. Phys. (A) Math. Gen.* 1981, **14**, L307
- 13 Drifford, M. and Dalbiez, J. P. *J. Phys. Chem.* 1984, **88**, 5368
- 14 Koene, R. S. and Mandel, M. *Macromolecules* 1983, **16**, 688; Koene, R. S., Nicolai, T. and Mandel, M. *Macromolecules* 1983, **16**, 227
- 15 Sedlak, M., Konak, C., Stepanek, P. and Jakes, J. *Polymer* 1987, **28**, 873
- 16 Schmidt, M. *Makromol. Chem., Rapid Commun.* 1989, **10**, 89
- 17 Schlager, H., Ph.D. Thesis, Universität Freiburg/Brsg, 1988
- 18 Schlager, H. and Burchard, W., personal communication
- 19 Nierlich, M., Williams, C. E., Boue, F., Cotton, J. P., Daoud, M., Farnoux, B., Jannink, G., Picot, C., Moan, M., Wolff, C., Rinaudo, M. and de Gennes, P. G. *J. Physique* 1979, **40**, 701
- 20 Nierlich, M., Boue, F., Lapp, A. and Oberthür, R. *Colloid Polym. Sci.* 1985, **263**, 955
- 21 Kanaya, T., Kaji, K., Kitamaru, R., Higgins, J. S. and Farago, B. *Macromolecules* 1989, **22**, 1356
- 22 Lin, S.-C., Lee, W. I. and Schurr, J. M. *Biopolymers* 1978, **17**, 1041
- 23 Nemoto, N., Matsuda, H., Tsunashima, Y. and Kurata, M. *Macromolecules* 1984, **17**, 1731
- 24 Ramsay, D. J. and Schmitz, K. *Macromolecules* 1985, **18**, 2422
- 25 Mathiez, P., Weisbuch, G. and Mouttet, C. *Biopolymers* 1979, **18**, 1465
- 26 Wilcoxon, J. P. and Schurr, J. M. *J. Chem. Phys.* 1983, **78**, 3354
- 27 Schmitz, K. S., Lu, M. and Gauntt, J. *J. Chem. Phys.* 1983, **78**, 5059
- 28 Drifford, M. and Dalbiez, J. P. *Biopolymers* 1985, **24**, 1501
- 29 Fuoss, R. M. *J. Polym. Sci.* 1948, **3**, 603
- 30 Fuoss, R. M. *J. Polym. Sci.* 1949, **4**, 96
- 31 Eisenberg, H. and Pouyet, J. *J. Polym. Sci.* 1954, **13**, 85
- 32 Cohen, J. and Priel, Z. *Macromolecules* 1989, **22**, 2356
- 33 Yamashita, Y., Shimizu, K., Nakao, Y., Choshi, H., Noda, I. and Nagasawa, M. *Polym. J.* 1986, **18**, 361
- 34 Förster, S., Diploma Thesis, Universität Mainz, 1989; Förster, S., Schmidt, M. and Antonietti, M., to be published
- 35 Förster, S., Kühn, A. and Schmidt, M., to be published
- 36 Siegert, A. J. F., MIT Rad. Lab. Rep. No. 465, 1943
- 37 Förster, S., Schmidt, M., Antonietti, M. and Lindner, P., to be published
- 38 Hayter, J. B., Jannink, G., Brochard-Wyart, F. and de Gennes, P. G. *J. Physique* 1980, **41**, L451
- 39 Koyama, R. *Physica (B)* 1983, **120**, 418
- 40 de Gennes, P. G. 'Scaling Concepts in Polymer Physics', Cornell University Press, Ithaca, NY, 1979
- 41 Fuoss, R. M. and Strauss, U. P. *J. Polym. Sci.* 1948, **3**, 246
- 42 Ackerson, B. J. *J. Chem. Phys.* 1976, **64**, 242
- 43 Ilmain, F. and Candau, S. J. *Macromolecules* submitted
- 44 Schaefer, D. W. *Science* 1989, **243**, 1023
- 45 Schmitz, K. and Ramsay, D. J. *Macromolecules* 1985, **18**, 933
- 46 Fulton, R. L. *J. Chem. Phys.* 1978, **68**, 3089, 3095
- 47 Fulton, R. L. *J. Chem. Phys.* 1983, **78**, 6865, 6877
- 48 Ise, N., Matsuoka, H. and Ito, K. *Macromolecules* 1989, **22**, 1